Materials Research Proceedings **2** (2016) 485-490 doi: http://dx.doi.org/10.21741/9781945291173-82

In-vitro Investigation of Air Plasma-Sprayed Hydroxyapatite Coatings by Diffraction Techniques

Ntsoane P. Tshepo[1, 2, a*], Theron Chris[1, b], Venter Andrew[2, c], Topic Mira[3, d], Härting Margit[4, e], Heimann Robert[5, f]

[1]Department of Physics, University of Pretoria, Pretoria, South Africa

[2]Research and Development Division, NECSA SOC Limited, Pretoria, South Africa

[3]Materials Research Department, iThemba LABS/National Research Foundation, Cape Town, South Africa

[4]Department of Physics, University of Cape Town, Cape Town, South Africa

[5]Am Stadtpark 2A, D-02826 Görlitz, Germany

[a]tshepo.ntsoane@necsa.co.za, [b]chris.theron@up.ac.za, [c]andrew.venter@necsa.co.za, [d]mtopic@tlabs.ac.za, [e]margit.harting@uct.ac.za, [f]robert.heimann@ocean-gate.de

Keywords: Plasma-Sprayed Hydroxyapatite Coatings, High-Energy Diffraction, Quantitative Phase Analysis, Depth-Resolved Residual Stress

Abstract. The influence exposure to simulated body fluid (SBF) has on plasma-sprayed hydroxyapatite (HAp) coatings of medical-grade Ti6Al4V rods was investigated by quantifying the depth dependence of the phase composition and residual stress through the coating thickness using diffraction techniques. Chemical phase identification showed HAp existing together with its thermal decomposition products, tetra-calcium phosphate (TTCP), tri-calcium phosphate (TCP) and calcium oxide. With depth, the HAp content decreases with a corresponding increase in TTCP. The near surface stress condition comprised ~50 ± 10 MPa hoop stress with the radial stress being close to zero. With depth the hoop stress decreases linearly to ~-50 ± 25 MPa at the substrate interface, whilst the radial stress increases with depth. Upon exposure to SBF, the coating composition reveals an increase in HAp from ~80.0 ± 0.5 to ~86.0 ± 0.5 wt%, accompanied by a decrease of TTCP from ~10 ± 2 to ~6 ± 2 wt% wt%. A change in stress state occurred within the first day of incubation; where after, with further exposure time the stress state converted back to values similar to that of the as-sprayed condition.

Introduction

The second-generation biomaterial hydroxyapatite (HAp), owing to its similarity to the inorganic component of bone, has been extensively studied as a candidate material in biomedical applications. Applications range from filling bone cavities [1] and artificial eye components [2] to coatings for hip endoprostheses and dental root implants for improved biological fixation [3]. However, the poor mechanical properties of the material limit its utilisation in fully load-bearing applications. In such cases, the material is applied as a coating on metallic substrates such as Ti, Ti alloys and CoCrMo, where the excellent mechanical properties of the metal are combined with the osseoconductive ability of the coating [4]. With the plethora of coating techniques available for deposition [5], thermal spray remains the method of choice on industrial scale [6]. It is known that the interaction of the high temperature droplets formed in the plasma, and subsequent rapid cooling on interaction with the cold substrates, leads to thermal decomposition. This causes the introduction of undesirable thermal decomposition products [7], such as TCP, TTCP, and sometimes calcium oxide. In addition it leads to a reduction in crystallinity [8]. These phases are known to be susceptible to dissolution in SBF [9]. This, together with stresses generated by the differential thermal mismatch (CTE) and quenching of

the droplets, may compromise the mechanical stability and integrity of the coating. Notwithstanding extensive investigations of the effect of incubation of HAp coatings in SBF [10], the bulk of the work focused on the near-surface region that has contact with living tissue. The present study deals with depth-resolved investigations of the effect that exposure to SBF has on HAp coatings.

Materials and Methods

Sample preparation. Hydroxyapatite powder (CAPTAL 90, batch P215, Plasma Biotal Limited, Tideswell, Derbyshire, UK), 120 ± 20 μm, was plasma-sprayed onto 7 mm diameter medical grade Ti6Al4V alloy rods supplied by Biomaterials Limited, North Yorkshire, UK. Details on the samples, HAp deposition procedure and spray parameters can be found in [11]. Coating thicknesses ranged from 150 to 180 μm. Subsequent to spraying, the samples were incubated for 1 and 7 days in a revised simulated body fluid (rSBF) based on Kokubo's formulation [12] to mimic the physiological environment with the solution temperature and pH kept at 36 °C and 7.4 respectively during the incubation period. The rSBF solution had an ionic concentration similar to that of human blood plasma, but free of non-collagenous proteins and enzymes. After incubation, disks approximately 5 mm in thickness were cut from the central part of the coated rod for investigation. The samples are shown in Fig. 1. Factors considered in determining the optimum disk thicknesses included minimization of the synchrotron beam attenuation, which, based on the energy of the beam and the mass absorption of the coating material was minimally influenced by the disk thickness, adequate diffracted intensities for good counting statistics, as well as limiting stress relaxation due to the cutting. Notwithstanding that the cutting would lead to relaxation of the axial stresses, due to the circular geometry, the hoop and radial stress components should not be influenced.

Through-thickness characterisation. High–energy synchrotron radiation, 70-130 keV, generated at the 3rd generation Advanced Photon Source's X-ray Operation and Research 6-ID-D beamline at Argonne National Laboratory (ANL), USA was used for the depth-resolved investigations of the phase composition and residual stresses. The experimental details and measurement procedure are reported in [11]. Measurements were done in transmission mode through the cut disks using an incident beam size of 0.035(V) x 0.400 (H) mm^2. The diffracted beams were recorded with an area detector located ~ 1m downstream. Supplementary near-surface investigations were carried out in reflection geometry, using a Bruker D8 Advance and a Discover instrument equipped with a Cu-anode that gave 8 keV energy X-rays that rendered ~0.015 mm penetration into HAp.

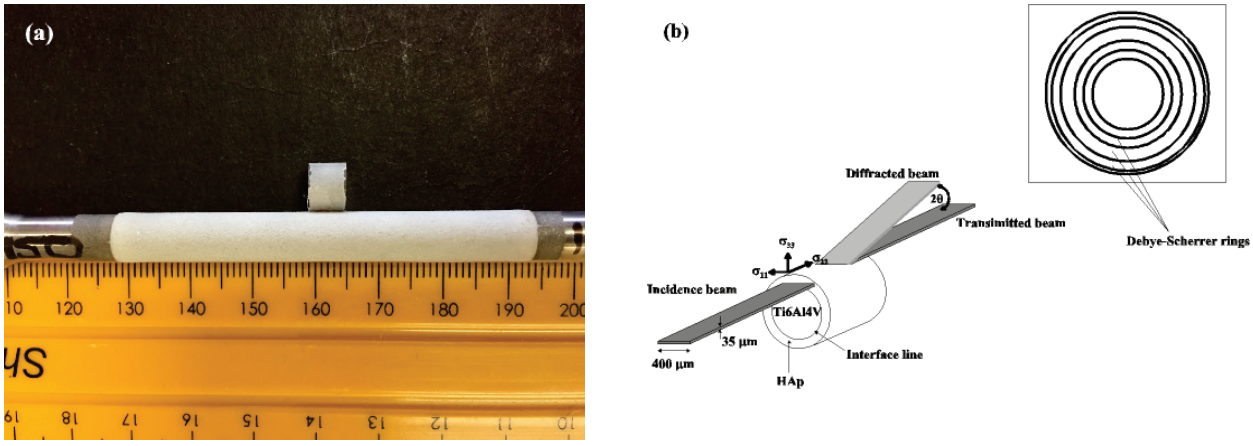

Figure 1: a) *Geometry and size of the HAp-coated (white) Ti6Al4V rod. Also shown is the cut disk; b) Schematic diagram illustrating the measurement geometry of the synchrotron beam in relation to the sample and the principal stress directions. This geometry in conjunction with an area detector enabled simultaneous measurement of the hoop (= σ_{11}) and radial (= σ_{33}) stress components at each depth.*

Materials Research Proceedings **2** (2016) 485-490 doi: http://dx.doi.org/10.21741/9781945291173-82

Results and discussion

Chemical phase analysis. Figure 2 shows diffraction patterns, displaced vertically for clarity, taken at different depths through the coating thickness from the as-sprayed and incubated samples. The phase determination shows the presence of the thermal decomposition products of HAp caused by the plasma temperature, being present throughout the coating thickness. The two top patterns, taken at the coating-substrate interface region, primarily show Ti6Al4V, indicate that the measurements extended up to the substrate. The CaO phase dissolved within the first week of incubation.

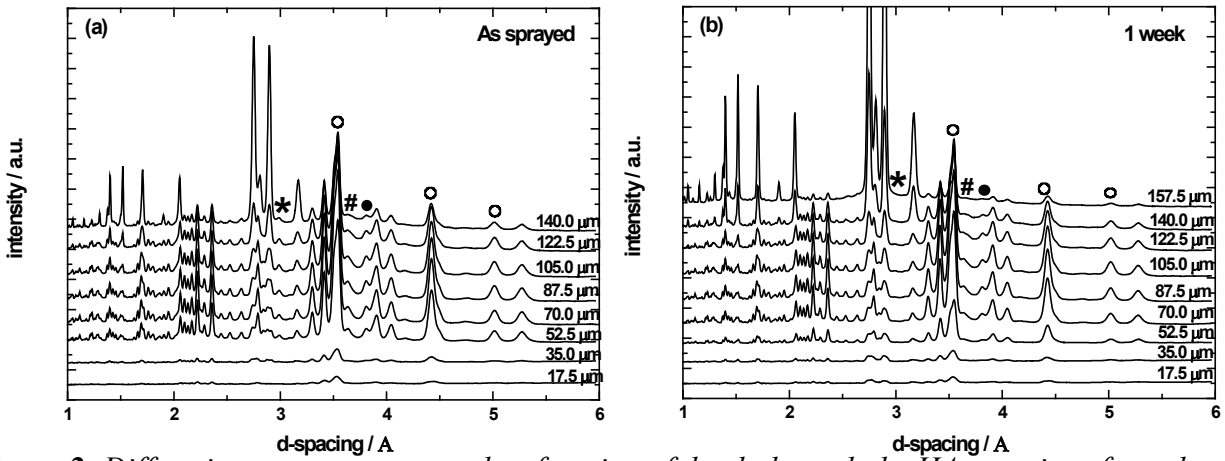

***Figure 2**: Diffraction patterns measured as function of depth through the HAp coatings from the coating surface (bottom pattern) to the substrate (top pattern) for: (a) As-sprayed and (b) Incubated for 1 week. The patterns show the presence of HAp (o), tetracalcium phosphate (#), tricalcium phosphate (•) and CaO (*). The diffraction patterns are displaced vertically for comparison purposes and respectively represent depth steps of 17.5µm*

Figure 3 shows the depth dependence of the primary phase, HAp, and the main thermal decomposition product, TTCP, for the as-sprayed and incubated samples. Also shown are their dependences as function of incubation times. Due to weak intensities from the coating, associated to the partial illumination of the coating, the first two diffraction patterns in Fig. 2 have been excluded in all analyses.

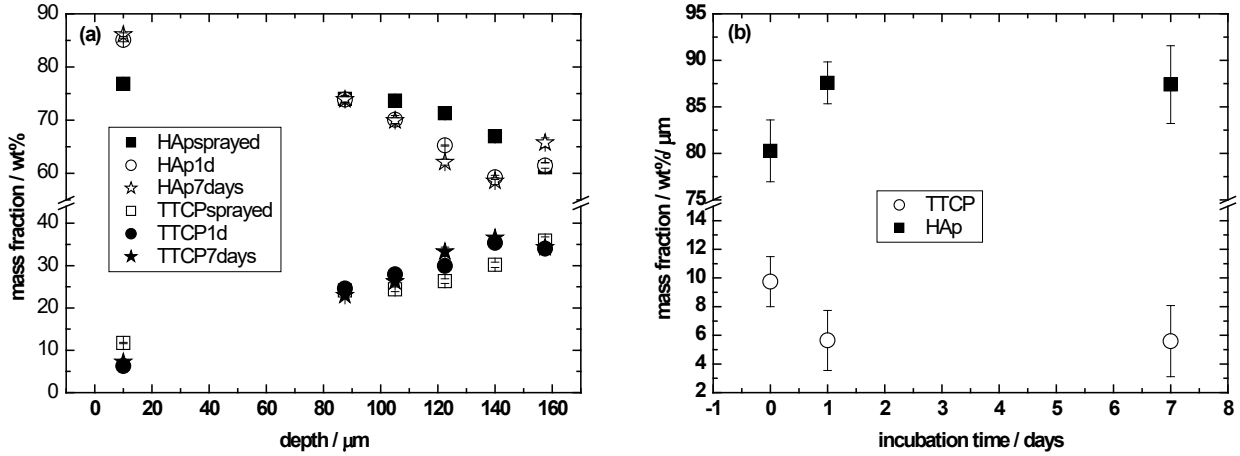

***Figure 3:** Variation of the chemical phase composition of the major phases (a) with depth and (b) with incubation time are shown for the as-sprayed and incubated samples, respectively.*

Materials Research Proceedings **2** (2016) 485-490 doi: http://dx.doi.org/10.21741/9781945291173-82

The HAp content of the as-sprayed coating (solid squares) systematically decrease with depth from 76 wt% to ~60 wt%. A similar trend is observed for the incubated samples where the HAp content decrease from ~86 to 62 wt% (open circles, open stars). The observed relative increase in HAp content with incubation time (Fig. 3b) can be attributed to the dissolution of thermal decomposition products, leaving the more stable HAp. Correspondingly, in the as-sprayed coating the TTCP phase (open squares) increases with depth from ~7 wt% to 35 wt%, whereas the incubated ones (solid dots, solid stars) increased from ~11 wt% to ~35 wt%. A cross-over point of the as-sprayed and incubated slopes occurs around mid-coating thickness. Although the preferential dissolution of TTCP in simulated body fluid has been widely reported [13], the results of this study indicate that this does not happen uniformly across the coating thickness. This implies that the solution only penetrates the surface region of the coating. The variation of the surface mass fraction with incubation time shown in Fig. 3, (right) reveals that the two phases show changes within the first day of incubation, with HAp increasing sharply from 80 wt% levelling off at ~86 wt% during further incubation; the opposite trend is observed for TTCP, decreasing from ~10 to ~6 wt% with time.

Residual stress profile

The HAp (213) diffraction peak was used to evaluate the residual strain. Assuming the Kroner-Eshelby grain interaction model, the X-ray elastic constants (XECs) $S_1\,(213) = -2.48 \cdot 10^{-6}$ MPa^{-1} and $½S_2\,(213) = 11.5 \cdot 10^{-6}$ MPa^{-1} [14] were used for the stress determination. Since only one azimuth orientation was measured, the stress components σ_{11}(= hoop), and σ_{33} (= radial) could be determined from the respectively measured d-values; the axial component, σ_{22} couldn't be determined with the measurement geometry. The stress-free reference value for strain determination was obtained from measurement of the starting powder. The d-spacing in the starting powder and ground coating flakes were within ± 0.00005 Å that correlates to ± 5.00 MPa stress uncertainty. The quantity (σ_{11}-σ_{33}), called the stress amplitude, is a useful parameter to consider since it is independent of possible sample misalignment contributions. The observed stress distribution comprises the accumulated effects of droplet quenching (also known as intrinsic stress), differential thermal mismatch between the coating and substrate, and stresses arising from possible volume changes due to phase transformations. Figure 4 summarises the depth distribution of the residual stress components and associated stress amplitude.

The results show that the hoop stress in the as-sprayed condition does not exceed 50 ± 10 MPa on the surface, whereas the radial stress is close to zero. The hoop stress steadily decreases with depth crossing the zero stress level around the coating mid-point to become ~ -50 ± 25 MPa compressive at the substrate interface. The radial stress steadily becomes tensile with depth reaching a maximum ~ 40 MPa at 157.5μm. Based on the intensities of diffraction patterns in Fig2, the measurements at 17.5, and 35 microns were carried out with only partially submerged beam hence the stress values at these depths are considered artefacts and therefore excluded; the same effect is expected at 175 and possibly at 157.5 microns. This effect in addition to possible relaxation and or overlapping substrate peak can be attributed to the observed large scatter at the interface. The observed radial stress distribution is consistent with previous synchrotron results and FEM analyses [15] which showed in general small tensile radial stresses near the surface region that increased with depth. The distribution can be attributed to various factors, including thermal gradient effects across the coating thickness during deposition [16], quenching stresses and effects associated with different inter-laminar bonding, intra-laminar micro-cracking, and pores.

Upon incubation, a change in stress state is observed in the hoop component. It becomes compressive on the surface and decreases with depth, i.e. an opposite trend to that of the as-coated condition. With further incubation, it reverts back to a trend similar to the as-sprayed condition. The radial component remains unaffected except at the interface region. The observed change in stress state during incubation can be attributed to the volume change based on the dissolution of thermal

decomposition products and onset of formation of an apatite-like octocalcium phosphate phase, with the former resulting from the existence of an ionic concentration gradient and the latter due to precipitation that forms due to supersaturation of the simulated body fluid with Ca2+ and HPO42- ions, respectively. Although Nimkerdphol et al. [17] observed an opposite stress state, a similar behaviour upon incubation was observed.

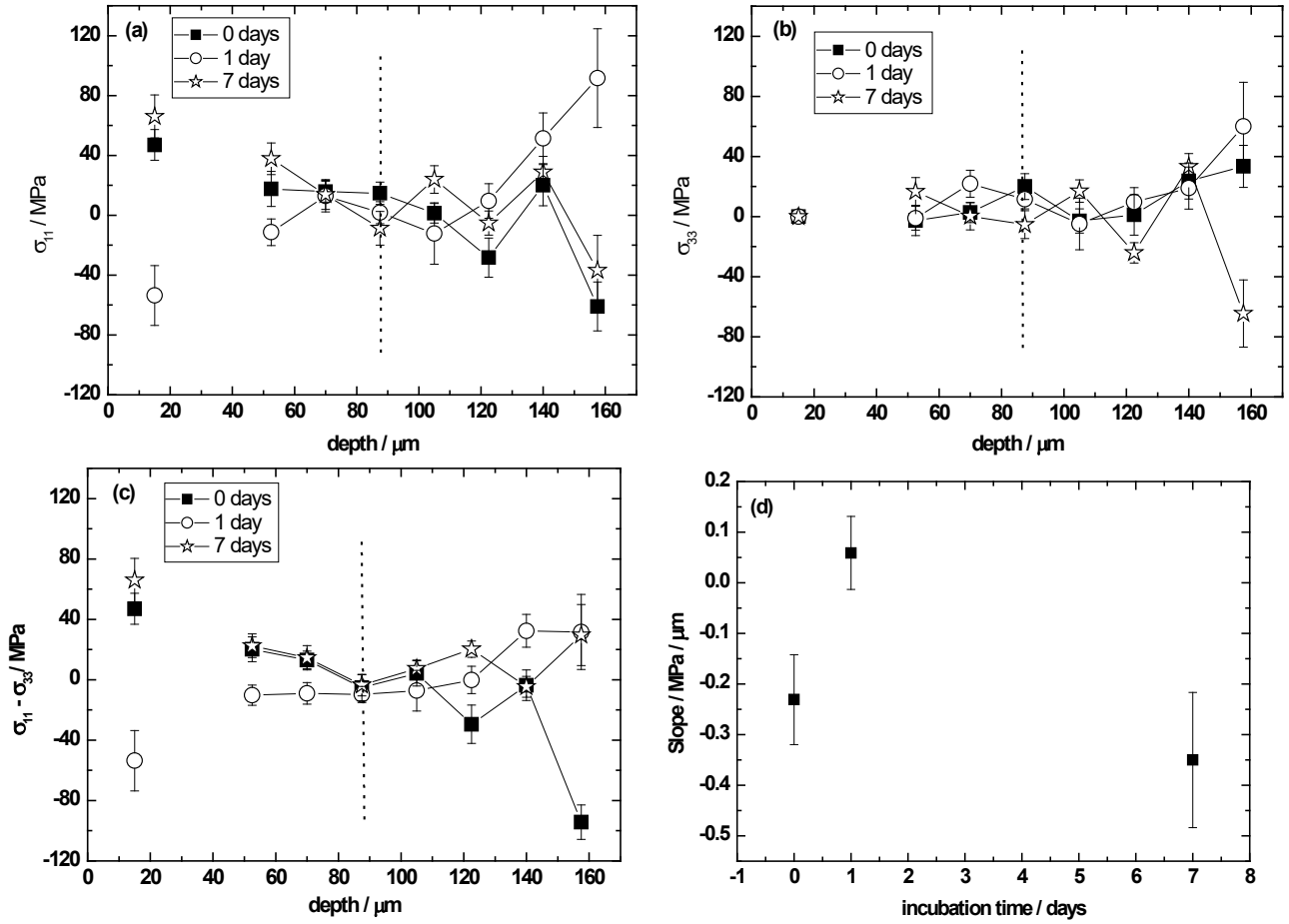

Figure 4: *Behaviour of the principal residual stress components with depth and incubation time, respectively for: (a) hoop, σ_{11}; (b) radial, σ_{33}; (c) σ_{11}-σ_{33}; and (d) average through-thickness stress gradient with incubation time.*

Conclusions

Depth-resolved in-vitro studies employing conventional X-ray and synchrotron radiation were carried out on air plasma-sprayed HAp coatings that revealed the following:

Phase identification results showed thermal decomposition products to be present throughout the as-sprayed condition with CaO dissolving completely within 7 days of incubation. Quantitative Rietveld analyses showed a near linear decrease of HAp with depth from ~76 ± 1 to ~60 ± 1 wt% with a corresponding linear increase of TTCP from ~7 ± 2 to ~35 ± 2 wt% for as-sprayed coatings. A similar trend was observed for samples incubated between 1 and 7 days in that HAp decreased with depth from ~86 ± 1 to ~62 ± 1 wt% and TTCP increased from ~11 ± 2 to ~35± 2 wt%. The coating composition as a function of immersion time reveals a steep increase of HAp from ~80 ± 0.5 to a constant ~86 ± 0.5 wt%, accompanied by a decrease of TTCP from ~10 ± 2 to ~6 ± 2 wt%.

The as-sprayed condition revealed that the hoop stress varied linearly from a tensile value at the surface to compressive at the substrate interface. The radial component is low at the surface and steadily increases to a maximum tensile value of ~ 30 MPa at 157 μm. The observed change in stress

state, of the hoop component, upon immersion into simulated body fluid can be attributed to both dissolution and onset of bone-like apatite precipitate, octacalcium phosphate.

Acknowledgements
Use of the 6-ID-D beamline at Argonne National Laboratory (ANL) was supported by the U.S. DOE Contract No. DE-AC02-06CH11357. The authors are indebted to Mrs Margitta Hengst, Department of Mineralogy, Technische Universität Bergakademie Freiberg, Germany for sample preparation, Drs Douglas Robinson and Jonathan Almer, ANL/APS for assisting with the experimental set-up, data acquisition and analysis. The research was sponsored by the German Federal Ministry of Education and Research and the South African National Research Foundation within the research project "Characterisation and determination of residual stress in bioactive coatings and layered structure" (Project code 39.6.G0B.6.A).

References

[1] T. Yamamoto, T. Onga, T. Marui, K. Mizuno, J. Bone Joint Surg. (Br.), 82B (2000) 1117. http://dx.doi.org/10.1302/0301-620X.82B8.11194

[2] T. Colen, Ophthalmology, 107 (2000) 1889. http://dx.doi.org/10.1016/S0161-6420(00)00348-1

[3] R.G.T. Geesink, K. de Groot, C.P.A.T. Klein, Clin. Orthop. Relat. Res., 225 (1987) 147.

[4] K. de Groot, R. Geesink, C.P.A.T. Klein, P. Serekian, J. Biomed. Mater. Res., 21 (1987) 1375. http://dx.doi.org/10.1002/jbm.820211203

[5] R.B. Heimann, H.D. Lehmann, Bioceramic Coatings for Medical Implants. Trends and Techniques. Wiley-VCH, Weinheim, Germany. 2015. pp 467.

[6] M. Topić, T. Ntsoane, T. Hüttel, R.B. Heimann, Surf. Coat. Technol.,201(6) (2006) 3633. http://dx.doi.org/10.1016/j.surfcoat.2006.08.139

[7] Y.C. Yang, B.C. Wang, E. Chang, J.D. Wu, J. Mat. Sci.: Mater. Med., 6 (1995) 249. http://dx.doi.org/10.1007/BF00120267

[8] K.A. Gross, C.C. Berndt, H. Herman, J. Biomed. Mater. Res., 39 (1998) 407. http://dx.doi.org/10.1002/(SICI)1097-4636(19980305)39:3<407::AID-JBM9>3.0.CO;2-N

[9] P. Ducheyne, S. Radin, L. King, J. Biomed. Mater. Res., 27 (1993) 25. http://dx.doi.org/10.1002/jbm.820270105

[10] S. R. Radin, P. Ducheyne, J. Materials Science: Materials in Medicine, 3, 1992, 33. http://dx.doi.org/10.1007/BF00702942

[11] T.P. Ntsoane, M. Topic, M. Härting, R.B. Heimann, C. Theron, Surf. Coating Technol, 294 (2016) 153. http://dx.doi.org/10.1016/j.surfcoat.2016.03.045

[12] T. Kokubo, H. Kushitani, S. Sakka, T. Kitsugi, T. Yamamuro, J. Biomed. Mater. Res., 24 (1990) 721. http://dx.doi.org/10.1002/jbm.820240607

[13] L. Sun, C.C. Berndt, K.A. Khor, H.N. Cheang, K.A. Gross, J. Biomed. Mater. Res., 62(2) (2002) 228. http://dx.doi.org/10.1002/jbm.10315

[14] T.N. Gardner, J.C. Elliot, Z. Sklar, G.A.D. Briggs, J. Biomech., 25 (1992) 1265. http://dx.doi.org/10.1016/0021-9290(92)90282-6

[15] A. Manescu, G. Albertini, P. Fogarassy, A. Lodino, N. Markocsan, J. Neutron Research, 12 (2004) 147. http://dx.doi.org/10.1080/10238160410001734603

[16] L. Pawlowski, M. Vardelle, P. Fauchais, Thin Solid Films, 94 (1982) 307. http://dx.doi.org/10.1016/0040-6090(82)90492-8

[17] A.R. Nimkerdphol, Y. Otsuka, Y. Mutoh, J. Mech. Behaviour Biomed. Mater., 36 (2014) 98. http://dx.doi.org/10.1016/j.jmbbm.2014.04.007